CHAPTER

Lateral-Directional Dynamics

7

7.1 Response to controls

The procedures for investigating and interpreting the lateral-directional dynamics of an aeroplane are much the same as those used to deal with the longitudinal dynamics; thus they are not repeated at the same level of detail in this chapter. However, some aspects of lateral-directional dynamics, and their interpretation, differ significantly from those of longitudinal dynamics, and the procedures for interpreting the differences are dealt with appropriately. The lateral-directional response transfer functions are obtained in the solution of the lateral equations of motion using, for example, the methods described in Chapter 5. The transfer functions completely describe the linear dynamic asymmetric response in sideslip, roll, and yaw to aileron and rudder inputs. As in the longitudinal solution, implicit in the response are the dynamic properties determined by the lateral-directional stability characteristics of the aeroplane. As before, the transfer functions and the response variables described by them are linear since the entire modelling process is based on the assumption that the motion is constrained to small disturbances about an equilibrium trim state. The equilibrium trim state is assumed to mean steady level flight in the first instance, and the previously stated caution concerning the magnitude of a small lateral-directional perturbation applies.

The most obvious difference between the solutions of the longitudinal equations of motion and the lateral−directional equations of motion is that there is more algebra to deal with. Since two aerodynamic inputs are involved, the ailerons and the rudder, two sets of input-output response transfer functions are produced in the solution of the equations of motion. However, these are no more difficult to deal with than a single input-output set of transfer functions; there are just more of them! The most significant difference between the longitudinal and lateral-directional dynamics of the aeroplane concerns interpretation. In general, the lateral-directional stability modes are not so distinct and tend to exhibit dynamic coupling to a greater extent. Thus some care is needed in the choice of assumptions made to facilitate their interpretation. A mitigating observation is that, unlike longitudinal dynamics, lateral-directional dynamics do not change much with flight condition since most aeroplanes possess aerodynamic symmetry by design.

The lateral-directional equations of motion describing small perturbations about an equilibrium trim condition, referred to wind axes, are given by the state equation (4.70) as follows:

$$\begin{bmatrix} \dot{v} \\ \dot{p} \\ \dot{r} \\ \dot{\phi} \end{bmatrix} = \begin{bmatrix} y_v & y_p & y_r & y_\phi \\ l_v & l_p & l_r & l_\phi \\ n_v & n_p & n_r & n_\phi \\ 0 & 1 & 0 & 0 \end{bmatrix} \begin{bmatrix} v \\ p \\ r \\ \phi \end{bmatrix} + \begin{bmatrix} y_\xi & y_\zeta \\ l_\xi & l_\zeta \\ n_\xi & n_\zeta \\ 0 & 0 \end{bmatrix} \begin{bmatrix} \xi \\ \zeta \end{bmatrix} \tag{7.1}$$

The solution of equation (7.1) produces two sets of four response transfer functions, one set describing motion in response to aileron input and a second set describing response to rudder input. As for the longitudinal response transfer functions, it is convenient to adopt a shorthand style of writing them. The transfer functions describing response to aileron are conveniently written as

$$\frac{v(s)}{\xi(s)} \equiv \frac{N_\xi^v(s)}{\Delta(s)} = \frac{k_v\left(s+1/T_{\beta_1}\right)\left(s+1/T_{\beta_2}\right)}{\left(s+1/T_s\right)\left(s+1/T_r\right)(s^2+2\zeta_d\omega_d s+\omega_d^2)} \tag{7.2}$$

$$\frac{p(s)}{\xi(s)} \equiv \frac{N_\xi^p(s)}{\Delta(s)} = \frac{k_p s(s^2+2\zeta_\phi\omega_\phi s+\omega_\phi^2)}{\left(s+1/T_s\right)\left(s+1/T_r\right)(s^2+2\zeta_d\omega_d s+\omega_d^2)} \tag{7.3}$$

$$\frac{r(s)}{\xi(s)} \equiv \frac{N_\xi^r(s)}{\Delta(s)} = \frac{k_r\left(s+1/T_\psi\right)(s^2+2\zeta_\psi\omega_\psi s+\omega_\psi^2)}{\left(s+1/T_s\right)\left(s+1/T_r\right)(s^2+2\zeta_d\omega_d s+\omega_d^2)} \tag{7.4}$$

$$\frac{\phi(s)}{\xi(s)} \equiv \frac{N_\xi^\phi(s)}{\Delta(s)} = \frac{k_\phi(s^2+2\zeta_\phi\omega_\phi s+\omega_\phi^2)}{\left(s+1/T_s\right)\left(s+1/T_r\right)(s^2+2\zeta_d\omega_d s+\omega_d^2)} \tag{7.5}$$

and the transfer functions describing response to rudder are conveniently written as

$$\frac{v(s)}{\zeta(s)} \equiv \frac{N_\zeta^v(s)}{\Delta(s)} = \frac{k_v\left(s+1/T_{\beta_1}\right)\left(s+1/T_{\beta_2}\right)\left(s+1/T_{\beta_3}\right)}{\left(s+1/T_s\right)\left(s+1/T_r\right)(s^2+2\zeta_d\omega_d s+\omega_d^2)} \tag{7.6}$$

$$\frac{p(s)}{\zeta(s)} \equiv \frac{N_\zeta^p(s)}{\Delta(s)} = \frac{k_p s\left(s+1/T_{\phi_1}\right)\left(s+1/T_{\phi_2}\right)}{\left(s+1/T_s\right)\left(s+1/T_r\right)(s^2+2\zeta_d\omega_d s+\omega_d^2)} \tag{7.7}$$

$$\frac{r(s)}{\zeta(s)} \equiv \frac{N_\zeta^r(s)}{\Delta(s)} = \frac{k_r\left(s+1/T_\psi\right)(s^2+2\zeta_\psi\omega_\psi s+\omega_\psi^2)}{\left(s+1/T_s\right)\left(s+1/T_r\right)(s^2+2\zeta_d\omega_d s+\omega_d^2)} \tag{7.8}$$

$$\frac{\phi(s)}{\zeta(s)} \equiv \frac{N_\zeta^\phi(s)}{\Delta(s)} = \frac{k_\phi\left(s+1/T_{\phi_1}\right)\left(s+1/T_{\phi_2}\right)}{\left(s+1/T_s\right)\left(s+1/T_r\right)(s^2+2\zeta_d\omega_d s+\omega_d^2)} \tag{7.9}$$

The solution of the equations of motion results in polynomial descriptions of the transfer function numerators and common denominator as set out in Appendix 3. The polynomials factorise into real and complex pairs of roots that are most explicitly quoted in the style of equations (7.2)–(7.9). Since the roots are interpreted as time constants, damping ratios, and natural frequencies, this style makes the essential information instantly available. It should also be noted that the numerator and denominator factors are typical for a conventional aeroplane. Sometimes pairs of complex roots may be replaced with two real roots and vice versa. However, this does not usually mean that the dynamic response characteristics of the aeroplane become dramatically different. Differences in the interpretation of response may be evident but are not necessarily large.

Transfer functions (7.2) through (7.9) each describe uniquely different, but related, variables in the motion of the aeroplane in response to a control input. However, it will be observed that the

notation adopted indicates similar values for some numerator terms in both aileron and rudder response transfer functions. For example, k_r, T_ψ, ζ_ψ, and ω_ψ appear in both $N^r_\xi(s)$ and $N^r_\zeta(s)$. **It must be understood that the numerator parameters are context-dependent and usually have a numerical value which is unique to the transfer function in question.** To repeat the comment made previously, the notation is a convenience for allocating particular numerator terms, and it serves only to identify the role of each term as a gain, time constant, damping ratio, or frequency.

As before, the denominator of the transfer functions describes the characteristic polynomial, which in turn describes the lateral-directional stability characteristics of the aeroplane. The transfer function denominator is therefore common to all response transfer functions. Thus the response of all variables to an aileron or a rudder input is dominated by the denominator parameters—namely, time constant, damping ratio, and natural frequency. The differences between the individual responses are entirely determined by their respective numerators, and the *response shapes* of the individual variables are determined by the common denominator and "coloured" by their respective numerators.

EXAMPLE 7.1

The equations of motion and aerodynamic data for the Douglas DC-8 aircraft were obtained from Teper (1969). At the flight condition of interest, the aircraft has a total weight of 190,000 Lb and is flying at Mach 0.44 at an altitude of 15,000 ft. The source data are referenced to aircraft body axes and, for the purposes of this illustration, have been converted to a wind axes reference using the transformations given in Appendices 7 and 8. The equations of motion, referred to wind axes and quoted in terms of concise derivatives, are, in state space format

$$\begin{bmatrix} \dot{v} \\ \dot{p} \\ \dot{r} \\ \dot{\phi} \end{bmatrix} = \begin{bmatrix} -0.1008 & 0 & -468.2 & 32.2 \\ -0.00579 & -1.232 & 0.397 & 0 \\ 0.00278 & -0.0346 & -0.257 & 0 \\ 0 & 1 & 0 & 0 \end{bmatrix} \begin{bmatrix} v \\ p \\ r \\ \phi \end{bmatrix} + \begin{bmatrix} 0 & 13.48416 \\ -1.62 & 0.392 \\ -0.01875 & -0.864 \\ 0 & 0 \end{bmatrix} \begin{bmatrix} \xi \\ \zeta \end{bmatrix} \quad (7.10)$$

Since it is useful to have the transfer function describing sideslip angle β as well as sideslip velocity v, the output equation is augmented as described in Section 5.7. Thus the output equation is

$$\begin{bmatrix} v \\ p \\ r \\ \phi \\ \beta \end{bmatrix} = \begin{bmatrix} 1 & 0 & 0 & 0 \\ 0 & 1 & 0 & 0 \\ 0 & 0 & 1 & 0 \\ 0 & 0 & 0 & 1 \\ 0.00214 & 0 & 0 & 0 \end{bmatrix} \begin{bmatrix} v \\ p \\ r \\ \phi \end{bmatrix} \quad (7.11)$$

Again, the numerical values of the matrix elements in equations (7.10) and (7.11) have been rounded to five decimal places in order to keep the equations to a reasonable written size. This should not be done with the equations used in the actual computation.

Solution of the equations of motion using Program CC produced the following two sets of transfer functions. First, the transfer functions describing response to aileron are as follows:

$$\begin{aligned}
\frac{v(s)}{\xi(s)} &= \frac{8.779(s+0.197)(s-7.896)}{(s+0.0065)(s+1.329)(s^2+0.254s+1.433)} \text{ ft/s/rad} \\
\frac{p(s)}{\xi(s)} &= \frac{-1.62s(s^2+0.362s+1.359)}{(s+0.0065)(s+1.329)(s^2+0.254s+1.433)} \text{ rad/s/rad (deg/s/deg)} \\
\frac{r(s)}{\xi(s)} &= \frac{-0.0188(s+1.59)(s^2-3.246s+4.982)}{(s+0.0065)(s+1.329)(s^2+0.254s+1.433)} \text{ rad/s/rad (deg/s/deg)} \\
\frac{\phi(s)}{\xi(s)} &= \frac{-1.62(s^2+0.362s+1.359)}{(s+0.0065)(s+1.329)(s^2+0.254s+1.433)} \text{ rad/rad (deg/deg)} \\
\frac{\beta(s)}{\xi(s)} &= \frac{0.0188(s+0.197)(s-7.896)}{(s+0.0065)(s+1.329)(s^2+0.254s+1.433)} \text{ rad/rad (deg/deg)}
\end{aligned} \tag{7.12}$$

Second, the transfer functions describing response to rudder are as follows:

$$\begin{aligned}
\frac{v(s)}{\zeta(s)} &= \frac{13.484(s-0.0148)(s+1.297)(s+30.207)}{(s+0.0065)(s+1.329)(s^2+0.254s+1.433)} \text{ ft/s/rad} \\
\frac{p(s)}{\zeta(s)} &= \frac{0.392s(s+1.85)(s-2.566)}{(s+0.0065)(s+1.329)(s^2+0.254s+1.433)} \text{ rad/s/rad (deg/s/deg)} \\
\frac{r(s)}{\zeta(s)} &= \frac{-0.864(s+1.335)(s^2-0.03s+0.109)}{(s+0.0065)(s+1.329)(s^2+0.254s+1.433)} \text{ rad/s/rad (deg/s/deg)} \\
\frac{\phi(s)}{\zeta(s)} &= \frac{0.392(s+1.85)(s-2.566)}{(s+0.0065)(s+1.329)(s^2+0.254s+1.433)} \text{ rad/rad (deg/deg)} \\
\frac{\beta(s)}{\zeta(s)} &= \frac{0.029(s-0.0148)(s+1.297)(s+30.207)}{(s+0.0065)(s+1.329)(s^2+0.254s+1.433)} \text{ rad/rad (deg/deg)}
\end{aligned} \tag{7.13}$$

The characteristic equation is given by equating the denominator to zero:

$$\Delta(s) = (s+0.0065)(s+1.329)(s^2+0.254s+1.433) = 0 \tag{7.14}$$

The first real root describes the spiral mode with time constant

$$T_s = \frac{1}{0.0065} \cong 154 \text{ s}$$

The second real root describes the roll subsidence mode with time constant

$$T_r = \frac{1}{1.329} = 0.75 \text{ s}$$

The pair of complex roots describe the oscillatory dutch roll mode with the following characteristics:

Damping ratio $\zeta_d = 0.11$
Undamped natural frequency $\omega_d = 1.2$ rad/s

Since both real roots are negative and the pair of complex roots have negative real parts, the mode characteristics indicate the airframe to be aerodynamically stable.

The response of the aeroplane to a unit (1 deg) aileron pulse, held for two seconds and then returned to zero, is shown in Fig. 7.1. All of the variables obtained in the solution of the equations of motion are shown, the individual responses being characterised by the transfer functions, equations (7.12).

The dynamics associated with the three stability modes are visible in the responses, although at first glance they appear to be dominated by the oscillatory dutch roll mode since its damping is relatively low. Because the non-oscillatory spiral and roll modes are not so distinct, and because the dynamic coupling between modes is significant, it is rather more difficult to expose the modes analytically unless some care is taken in their graphical presentation. This subject is discussed in greater detail in Section 7.6. Both the roll and spiral modes appear as exponentially convergent characteristics since they are both stable in this example. The roll mode converges relatively quickly with a time constant of 0.75 s, whereas the spiral mode converges very slowly indeed with a time constant of 154 s. The roll mode is most clearly seen in the roll rate response p, where it determines the exponential rise at 0 s and the exponential recovery when the pulse is removed at 2 s. The spiral mode characteristic is rather more subtle and is most easily seen in the roll attitude response ϕ, where it determines the longer term convergence to zero and is fully established at 30 s.

Once again, all of the response shapes are determined by the common stability mode dynamics, and the obvious differences between them are due to the unique numerators in each transfer function. All of the response variables shown in Fig. 7.1 eventually decay to zero in the time scale of the spiral mode (about 200 seconds) since the aircraft is stable.

The response of the aeroplane to a unit (1°) rudder step input is shown in Fig. 7.2. All of the variables obtained in the solution of the equations of motion are shown, the individual responses being characterised by the transfer functions, equations (7.13). Again, it is very clear that the response is dominated by the oscillatory dutch roll mode. However, unlike the previous illustration, the roll and spiral modes are not discernible in the response. This is due to the fact that a step was chosen as the input that simply causes the aircraft to diverge from its initial equilibrium. This motion, together with the dutch roll oscillation, effectively masks the two non-oscillatory modes.

Now, it is possible to observe another interesting phenomenon in the response. Inspection of the transfer functions, equations (7.12) and (7.13), reveals that a number possess non-minimum phase numerator terms. The effect of these non-minimum phase terms would seem to be insignificantly small since they are not detectable in the responses shown in Figs 7.1 and 7.2, with one exception. The roll rate response p to rudder, shown in Fig. 7.2, exhibits a sign reversal for the first second or so of its response; this is the manifestation of the non-minimum phase effect. In aeronautical parlance it is referred to as *adverse roll* in response to rudder.

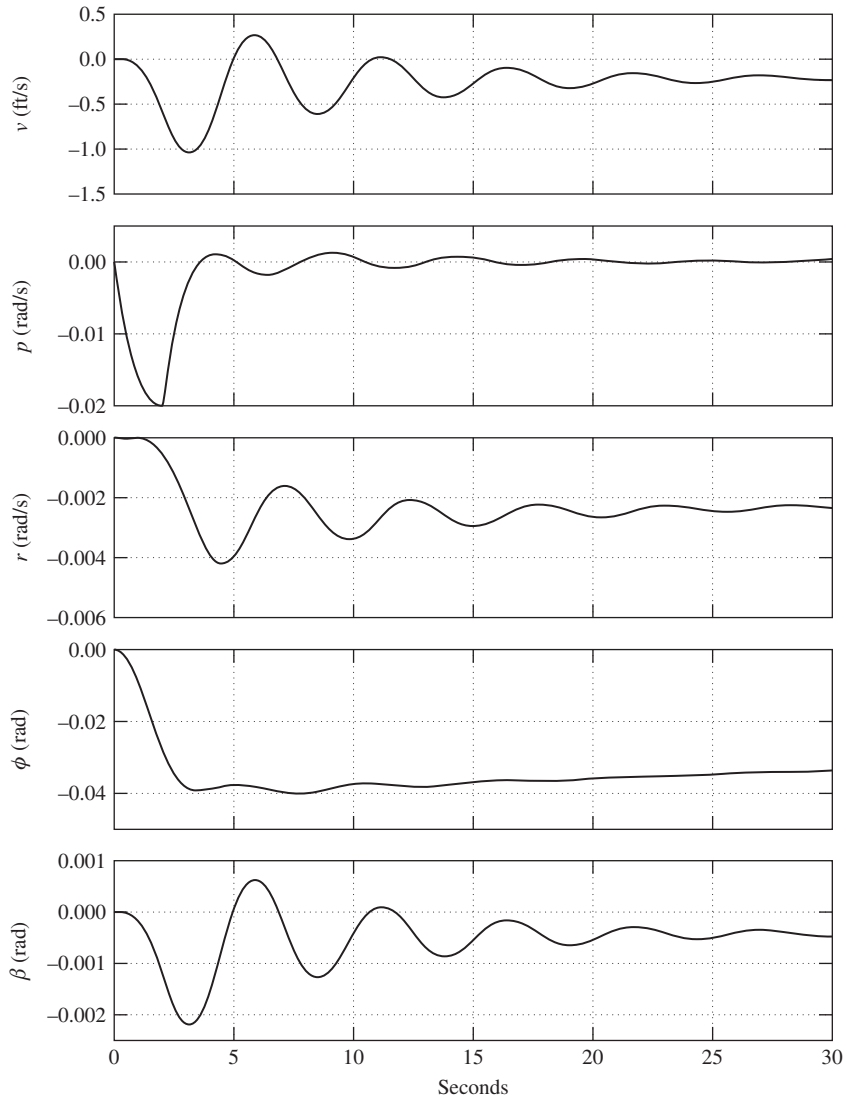

FIGURE 7.1 Aircraft response to a 1 deg, 2 s aileron pulse input.

A positive rudder step input is assumed that causes the aircraft to turn to the left, which is a negative response in accordance with the notation. Once the turn is established this results in negative yaw and yaw rate together with negative roll and roll rate induced by yaw-roll coupling. These general effects are correctly portrayed in the responses shown in Fig. 7.2. However,

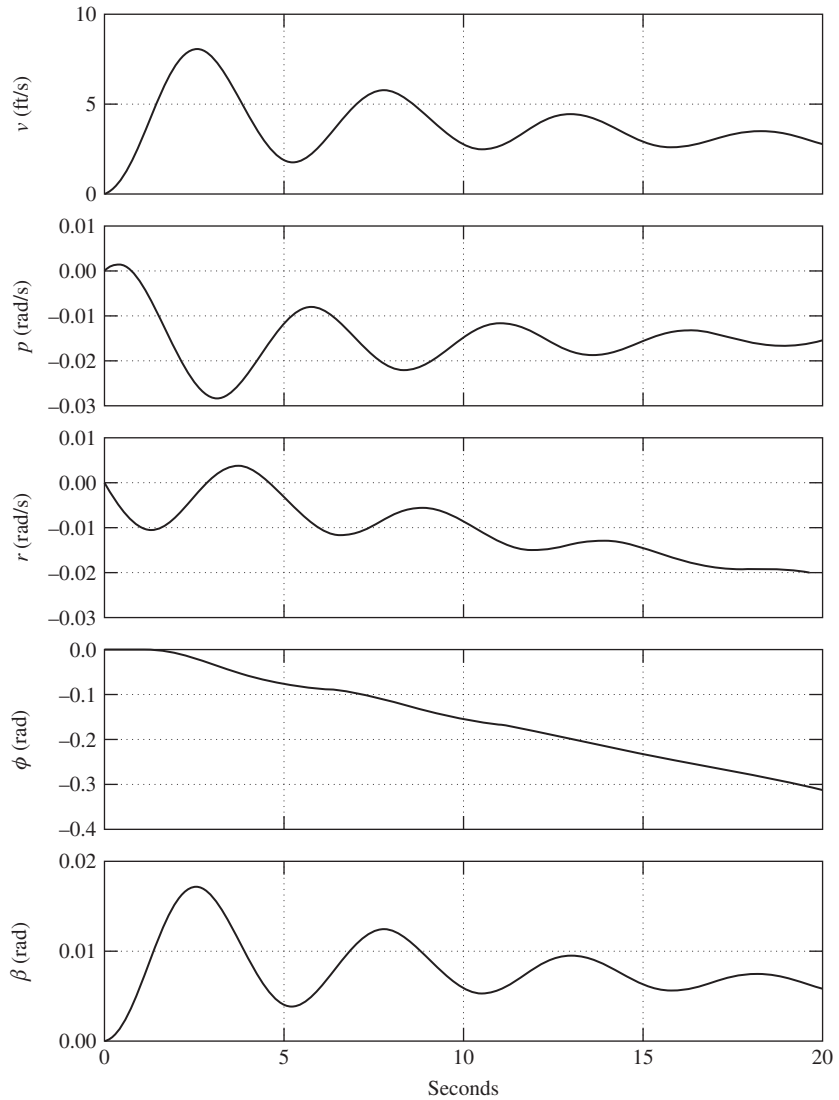

FIGURE 7.2 Aircraft response to a 1 deg rudder step input.

when the rudder is deflected, initially a substantial side force is generated at the centre of pressure of the fin, which in turn generates the yawing moment causing the aircraft to turn. However, the side force acts at some distance above the roll axis and also generates a rolling moment, which causes the aircraft to roll in the opposite sense to that induced by the yawing

motion. Since inertia in roll is somewhat lower than inertia in yaw, the aircraft responds quicker in roll and starts to roll in the "wrong" direction, but as the yawing motion becomes established the aerodynamically induced rolling moment eventually overcomes the adverse rolling moment and the aircraft then rolls in the "correct" sense.

This behaviour is clearly visible in Fig. 7.2 and is a characteristic found in most aircraft. The magnitude of the effect is aircraft dependent and, if not carefully controlled by design, can lead to unpleasant handling characteristics. A similar characteristic, *adverse yaw* in response to aileron, is caused by the differential drag effects associated with aileron deflection, giving rise to an adverse yawing moment. This characteristic is also commonly observed in many aircraft; reference to equations (7.12) indicates that it is present in the DC-8 but is insignificantly small at the chosen flight condition.

The mode content in each of the motion variables is given most precisely by the eigenvectors. The relevance of eigenvectors is discussed in Section 5.6, and the analytical procedure for obtaining them is illustrated in Example 5.7. With the aid of MATLAB, the eigenvector matrix $\mathbf{V}$ was obtained from the state matrix in equation (7.10):

$$\begin{array}{c} \qquad\qquad \text{dutch roll mode} \qquad\qquad\qquad\qquad \begin{array}{c}\text{roll}\\ \text{mode}\end{array} \quad \begin{array}{c}\text{spiral}\\ \text{mode}\end{array} \\ \mathbf{V} = \left[\begin{array}{cc:c:c} -0.845+0.5291j & -0.845-0.5291j & -0.9970 & 0.9864 \\ 0.0012-0.0033j & 0.0012+0.0033j & -0.0619 & -0.0011 \\ 0.0011+0.0021j & 0.0011-0.0021j & 0.0006 & 0.0111 \\ -0.0029-0.0007j & -0.0029+0.0007j & 0.0466 & 0.1641 \end{array}\right] \begin{array}{l} :\ v \\ :\ p \\ :\ r \\ :\ \phi \end{array} \end{array} \tag{7.15}$$

To facilitate interpretation of the eigenvector matrix, the magnitude of each component eigenvector is calculated as follows:

$$|\mathbf{V}| = \left[\begin{array}{cc:c:c} 0.9970 & 0.9970 & 0.9970 & 0.9864 \\ 0.0035 & 0.0035 & 0.0619 & 0.0011 \\ 0.0024 & 0.0024 & 0.0006 & 0.0111 \\ 0.0030 & 0.0030 & 0.0466 & 0.1641 \end{array}\right] \begin{array}{l} :\ v \\ :\ p \\ :\ r \\ :\ \phi \end{array}$$

Clearly, the content of all three modes in sideslip velocity v, and hence in β, is of similar order: The roll mode is dominant in roll rate p and the spiral mode is dominant in roll attitude response ϕ. These observations correlate well with the responses shown in Fig. 7.1 and Fig. 7.2, but the low dutch roll damping obscures the observation in some response variables. Although not the case in this example, eigenvector analysis can be particularly useful for interpreting lateral-directional response in aircraft where mode coupling is rather more pronounced and the modes are not so distinct.

The steady-state values of the motion variables following a unit step (1 deg) aileron or rudder input may be determined by the application of the final value theorem, equation (5.33), to the transfer functions, equations (7.12) and (7.13). (The calculation procedure is illustrated in

Example 6.1 and is not repeated here.) Thus the steady state response of all the motion variables to an aileron unit step input is

$$\begin{bmatrix} v \\ p \\ r \\ \phi \\ \beta \end{bmatrix}_{\substack{steady \\ state}} = \begin{bmatrix} -19.24 \text{ ft/s} \\ 0 \\ -11.99 \text{ deg/s} \\ -177.84 \text{ deg} \\ -2.35 \text{ deg} \end{bmatrix}_{aileron} \tag{7.16}$$

and the steady-state response to a rudder unit step input is

$$\begin{bmatrix} v \\ p \\ r \\ \phi \\ \beta \end{bmatrix}_{\substack{steady \\ state}} = \begin{bmatrix} -11.00 \text{ ft/s} \\ 0 \\ -10.18 \text{ deg/s} \\ -150.36 \text{ deg} \\ -1.35 \text{ deg} \end{bmatrix}_{rudder} \tag{7.17}$$

It must be realised that the steady-state values given in equations (7.16) and (7.17) serve only to give an indication of the control sensitivity of the aeroplane. At such large roll attitudes the small perturbation model ceases to apply and in practice significant changes in aerodynamic operating conditions would accompany the response. The actual steady state values are undoubtedly somewhat different and can be ascertained only with a full nonlinear simulation model. This illustration indicates the limiting nature of a small-perturbation model for the analysis of lateral-directional dynamics and the need to exercise care in its interpretation.

7.1.1 The characteristic equation

The lateral-directional characteristic polynomial for a classical aeroplane is fourth order; it determines the common denominator of the lateral and directional response transfer functions and, when equated to zero, defines the characteristic equation, which may be written as

$$As^4 + Bs^3 + Cs^2 + Ds + E = 0 \tag{7.18}$$

The characteristic equation (7.18) most commonly factorises into two real roots and a pair of complex roots, which are most conveniently written as

$$(s + 1/T_s)(s + 1/T_r)(s^2 + 2\zeta_d\omega_d s + \omega_d^2) = 0 \tag{7.19}$$

As indicated previously, the first real root in equation (7.19) describes the non-oscillatory spiral mode, the second real root describes the nonoscillatory roll subsidence mode, and the pair of complex roots describe the oscillatory dutch roll mode. Now, since the equations of motion from which the characteristic equation is derived are referred to wind axes, the stability modes comprising equation (7.19) provide a complete description of the lateral-directional stability properties of the aeroplane with respect to the total steady velocity vector and subject to the constraints of small-perturbation motion.

When the equations of motion are referred to a body axes system, the state equation (4.69) is fifth order, as is the characteristic equation. The solution of the characteristic equation then has the following factors:

$$s\left(s + 1/T_s\right)\left(s + 1/T_r\right)(s^2 + 2\zeta_d\omega_d s + \omega_d^2) = 0 \tag{7.20}$$

The modes are unchanged except for the addition of a zero root, which indicates neutral stability. The zero root results from the addition of yaw angle to the state equation and indicates neutral stability in yaw or heading. Interpretation of lateral-directional dynamics is unchanged, and the additional information indicates that the aeroplane has an indeterminate yaw or heading angle. In other words, lateral-directional dynamics are evaluated about the steady total velocity vector, which assumes an arbitrary direction in azimuth, yaw, or heading. Interpretation of the non-zero roots of the characteristic equation is most easily accomplished if reference is first made to the properties of the classical mass-spring-damper system, which are summarised in Appendix 6.

Unlike the longitudinal dynamics, interpretation of lateral-directional dynamics is not quite so straightforward because the stability modes are not as distinct; there usually exists a significantly greater degree of mode coupling, or interaction. This tends to make the necessary simplifying assumptions less appropriate, with a consequent reduction of confidence in the observations. However, an assortment of well tried procedures for interpreting the dynamic characteristics of the well behaved aeroplane exist, and these are discussed below.

The principal objective, of course, is to identify the aerodynamic drivers for each of the stability modes. The connection between the observed dynamics of the aeroplane and its aerodynamic characteristics is made by comparing equation (7.18) with either equation (7.19) or equation (7.20) and then referring to Appendix 3 for the definitions of the coefficients in equation (7.18) in terms of aerodynamic stability derivatives. It will be appreciated immediately that further analytical progress is impossibly difficult unless some gross simplifying assumptions are made. Dealing with this difficulty requires the derivation of reduced order models, as described in Section 7.3.

7.2 The dynamic stability modes

As for the longitudinal stability modes, whenever the aeroplane is disturbed from its equilibrium trim state the lateral-directional stability modes are also excited. Again, the disturbance may be initiated by pilot control action, a change in power setting, airframe configuration changes such as flap deployment, and external influences such as gusts and turbulence.

7.2.1 The roll subsidence mode

The *roll subsidence mode*, or simply *roll mode*, is a nonoscillatory lateral characteristic which is usually substantially decoupled from the spiral and dutch roll modes. Since it is nonoscillatory, it is described by a single real root of the characteristic polynomial, and manifests itself as an exponential lag characteristic in rolling motion. The aeromechanical principles governing the behaviour of the mode are illustrated in Fig. 7.3.

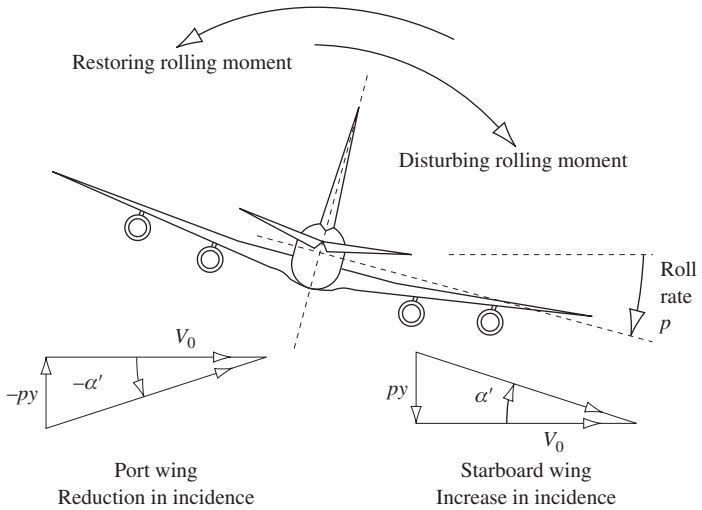

FIGURE 7.3 Roll subsidence mode.

With reference to Fig. 7.3, the aircraft is viewed from the rear, so the indicated motion is shown in the same sense as experienced by the pilot. Assume that the aircraft is constrained to single degree of freedom motion in roll about the *ox* axis only, and that it is initially in trimmed wings level flight. If the aeroplane experiences a positive disturbing rolling moment, it commences to roll with an angular acceleration in accordance with Newton's second law of motion. In rolling motion the wing experiences a component of velocity normal to the wing py, where y is the spanwise coordinate measured from the roll axis *ox*. As indicated in Fig. 7.3, this results in a small increase in incidence on the down-going starboard wing and a small decrease in incidence on the up-going port wing. The resulting differential lift gives rise to a restoring rolling moment as indicated. The corresponding resulting differential induced drag also gives rise to a yawing moment, but this is usually small enough to be ignored. Thus, following a disturbance the roll rate builds up exponentially until the restoring moment balances the disturbing moment and a steady roll rate is established.

In practice, of course, this kind of behaviour would be transient rather than continuous as implied in this illustration. The physical behaviour explained is simple "paddle" damping and is stabilising in effect in all aeroplanes operating in normal, aerodynamically linear flight regimes. For this reason, the stability mode is sometimes referred to as *damping in roll*.

In some modern combat aeroplanes designed to operate in seriously nonlinear aerodynamic conditions—for example, at angles of attack approaching 90 deg, it is possible for the physical conditions governing the roll mode to break down completely. The consequent loss of roll stability can result in rapid roll departure followed by complex lateral-directional motion of a hazardous nature. However, in the conventional aeroplane the roll mode appears to the pilot as a lag in roll response to controls. The lag time constant is largely dependent on the moment of inertia in roll and the aerodynamic properties of the wing, and is typically around 1 s or less.

7.2.2 The spiral mode

The *spiral mode* is also nonoscillatory and is determined by the other real root in the characteristic polynomial. When excited, the mode dynamics are usually slow to develop and involve complex coupled motion in roll, yaw, and sideslip. The dominant aeromechanical principles governing the mode dynamics are illustrated in Fig. 7.4. The mode characteristics are very dependent on the lateral static stability and the directional static stability of the aeroplane. These topics are discussed in Sections 3.4.1 and 3.4.2

The spiral mode is usually excited by a disturbance in sideslip, which typically follows a disturbance in roll and causes a wing to drop. Assume that the aircraft is initially in trimmed wings level flight and that a disturbance causes a small positive roll angle ϕ to develop. Left unchecked, this results in a small positive sideslip velocity v as indicated at (a) in Fig. 7.4. The sideslip puts the fin at incidence β, which produces lift and, in turn, generates a yawing moment to turn the aircraft into the direction of the sideslip. The yawing motion produces differential lift across the wing span, which in turn results in a rolling moment, causing the starboard wing to drop further thereby exacerbating the situation. This developing divergence is indicated at (b) and (c) in Fig. 7.4. Simultaneously, the dihedral effect of the wing generates a negative restoring rolling moment due to sideslip which acts to return the wing to a level attitude. Some additional restoring rolling moment is also generated by the fin lift force when it acts at a point above the roll axis ox, which is usual.

The situation is thus one in which the fin effect, or directional static stability, and the dihedral effect, or lateral static stability, act in opposition to create this interesting dynamic condition.

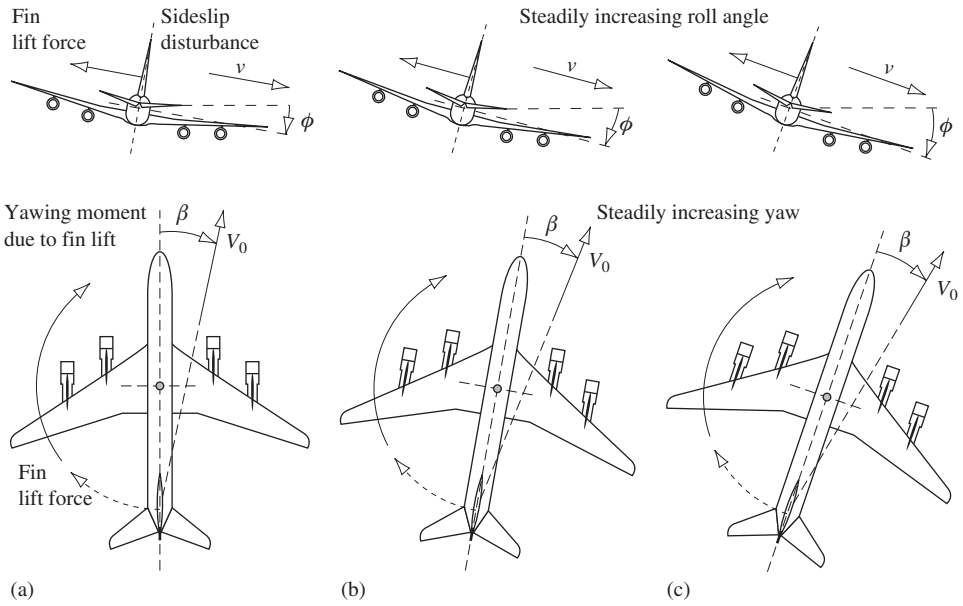

FIGURE 7.4 Spiral mode development.

Typically, the requirements for lateral and directional static stability are such that the opposing effects are very nearly equal. When the dihedral effect is greater, the spiral mode is stable and hence convergent; when the fin effect is greater, the spiral mode is unstable and hence divergent. Since these effects are nearly equal, the spiral mode is nearly neutrally stable, and sometimes it may even be neutrally stable—that is, it is neither convergent nor divergent. Since the mode is non-oscillatory, it manifests itself as a classical exponential convergence or divergence and, since it is nearly neutral, the time constant is very large, typically 100 s or more. This means that when the mode is stable the wing is slow to recover a level attitude following a disturbance, and when it is unstable the rate at which it diverges is also very slow. When it is neutral the aircraft simply flies a turn at constant roll attitude.

It is the unstable condition which attracts the most attention, for obvious reasons. Once the mode is excited the aircraft flies a slowly diverging path in both roll and yaw, and since the vertical forces are no longer in equilibrium the aircraft also loses height. Thus the unstable flight path is a spiral descent which, if left unchecked, ends when the aircraft hits the ground! However, since the rate at which the mode diverges is usually very slow, most pilots can cope with it. For this reason, an unstable spiral mode is permitted provided its time constant is sufficiently large. Because the mode is very slow to develop, the accelerations in the resulting motion are insignificantly small and the motion cues available to the pilot are almost imperceptible. In a spiral departure the visual cues become the most important cues to the pilot. It is also important to appreciate that a spiral departure is not the same as a spin. Spinning motion is a fully stalled flight condition, whereas in a spiral descent the wing continues to fly in the usual sense.

7.2.3 The dutch roll mode

The *dutch roll* mode is a classical damped oscillation in yaw, about the *oz* axis of the aircraft, which couples into roll and, to a lesser extent, into sideslip. The motion it describes is therefore a complex interaction between all three lateral-directional degrees of freedom. The characteristics of the dutch roll mode are described by the pair of complex roots in the characteristic polynomial. Fundamentally, the dutch roll mode is the lateral-directional equivalent of the longitudinal short-period mode. Since the moments of inertia in pitch and yaw are of similar magnitude, the frequency of the dutch roll mode and the longitudinal short-period mode are of similar order. However, the fin is generally less effective than the tailplane as a damper and the damping of the dutch roll mode is often inadequate. The dutch roll mode is so called because the motion of the aeroplane following its excitation is said to resemble the rhythmical flowing motion of a Dutch skater on a frozen canal. One cycle of typical dutch rolling motion is shown in Fig. 7.5.

The physical situation applying in a dutch roll disturbance can be appreciated by imagining that the aircraft is restrained in yaw by a torsional spring acting about the yaw axis *oz*, the spring stiffness being aerodynamic and determined largely by the fin. Thus, when in straight, level trimmed equilibrium flight, a disturbance in yaw causes the "aerodynamic spring" to produce a restoring yawing moment which results in classical oscillatory motion. However, once the yaw oscillation is established the relative velocity of the air over the port and starboard wings also varies in an oscillatory manner, giving rise to oscillatory differential lift and drag perturbations. This aerodynamic coupling in turn creates an oscillation in roll which lags the oscillation in yaw by approximately 90 deg. This phase difference between yawing and rolling motion means that the forward going wing

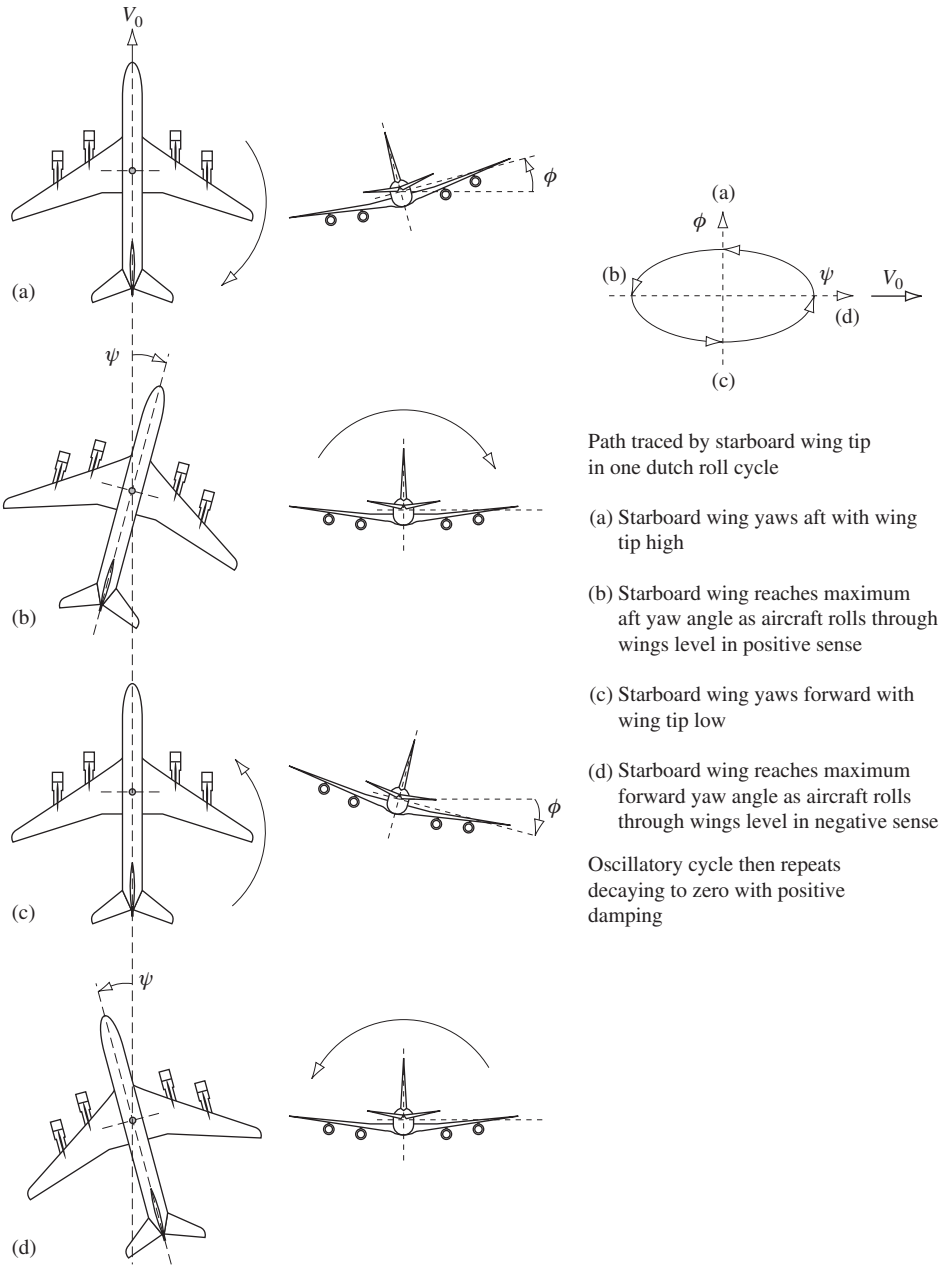

Path traced by starboard wing tip in one dutch roll cycle

(a) Starboard wing yaws aft with wing tip high

(b) Starboard wing reaches maximum aft yaw angle as aircraft rolls through wings level in positive sense

(c) Starboard wing yaws forward with wing tip low

(d) Starboard wing reaches maximum forward yaw angle as aircraft rolls through wings level in negative sense

Oscillatory cycle then repeats decaying to zero with positive damping

FIGURE 7.5 Oscillatory dutch roll mode.

panel is low and the aft going wing panel is high, as indicated in Fig. 7.5. Consequently, the classical manifestation of the dutch roll mode is given by the path described by the wing tips relative to the horizon and is usually elliptical, also as shown in Fig. 7.5. The ratio of peak roll to peak yaw is usually less than 1, as indicated, and is usually associated with a stable dutch roll mode. However, when the ratio is greater than 1 an unstable dutch roll mode is more likely.

Whenever the wing is disturbed from level trim, the aeroplane, left to its own devices, starts to slip sideways in the direction of the low wing. Thus the oscillatory rolling motion leads to some oscillatory sideslipping motion in dutch rolling motion, although the sideslip velocity is generally small. For this reason, it is fairly easy to build a visual picture of the complex interactions involved in the dutch roll mode. In fact, the motion experienced in a dutch rolling aircraft seems analogous to that of a ball bearing dropped into an inclined channel having a semicircular cross section. The ball bearing rolls down the inclined channel whilst oscillating from side to side on the circular surface.

Both the damping and stiffness in yaw, which determine the characteristics of the mode, are largely determined by the aerodynamic properties of the fin, a large fin being desirable for a well behaved stable dutch roll mode. Unfortunately, this contradicts the requirement for a stable spiral mode. The resulting aerodynamic design compromise usually results in aeroplanes with a mildly unstable spiral mode and a poorly damped dutch roll mode. Of course, the complexity of the dynamics associated with this mode suggests that there must be other aerodynamic contributions to the mode characteristics in addition to the fin. This is generally the case, and it is quite possible for the additional aerodynamic effects to be as significant as the aerodynamic properties of the fin, if not more so. However, one thing is quite certain: It is very difficult to quantify all aerodynamic contributions to the dutch roll mode with any degree of confidence.

7.3 Reduced order models

Unlike the longitudinal equations of motion, it is more difficult to solve the lateral-directional equations of motion approximately. Because of the motion coupling present, to a greater or lesser extent, in all three modes dynamics, the modes are not so distinct and simplifying approximations are thus less relevant, with a consequent loss of accuracy. Response transfer functions derived from reduced order models based on simplified approximate equations of motion are generally insufficiently accurate to be of any real use other than to enhance understanding of the aeromechanics of lateral-directional motion.

The simplest, and most approximate, solution of the characteristic equation provides an initial estimate for the two real roots only. This approximate solution of the lateral-directional characteristic equation (7.18) is based on the observation that conventional aeroplanes give rise to coefficients A, B, C, D, and E that have relative values which do not change very much with flight condition. Typically, A and B are relatively large whilst D and E are relatively small; in fact, E is often close to zero. Further, it is observed that $B >> A$ and $E << D$ suggesting the following real roots as approximate solutions of the characteristic equation:

$$\begin{aligned}(s + 1/T_r) &\cong (s + B/A)\\ (s + 1/T_s) &\cong (s + E/D)\end{aligned} \tag{7.21}$$

No such simple approximation for the pair of complex roots describing the dutch roll mode may be determined. Further insight into the aerodynamic drivers governing the characteristics of the roll and spiral modes may be made, with some difficulty, by applying assumptions based on the observed behaviour of the modes to the polynomial expressions for A, B, D, and E given in Appendix 3. Fortunately, the same information may be deduced by a rather more orderly process involving a reduction in order of the equations of motion. The approximate solutions for the nonoscillatory modes as given by equations (7.21) are only useful for preliminary mode evaluations, or for checking computer solutions, when the numerical values of the coefficients in the characteristic equation are known.

7.3.1 The roll mode approximation

Provided that the perturbation is small, the roll subsidence mode is observed to involve almost pure rolling motion with little coupling into sideslip or yaw. Thus a reduced order model of the lateral-directional dynamics retaining only the roll mode follows by removing the side force and yawing moment equations from the lateral-directional state equation (7.1):

$$\begin{bmatrix} \dot{p} \\ \dot{\phi} \end{bmatrix} = \begin{bmatrix} l_p & l_\phi \\ 1 & 0 \end{bmatrix} \begin{bmatrix} p \\ \phi \end{bmatrix} + \begin{bmatrix} l_\xi & l_\zeta \\ 0 & 0 \end{bmatrix} \begin{bmatrix} \xi \\ \zeta \end{bmatrix} \tag{7.22}$$

Further, if aircraft wind axes are assumed, then $l_\phi = 0$ and equation (7.22) reduces to the single degree of freedom rolling moment equation,

$$\dot{p} = l_p p + l_\xi \xi + l_\zeta \zeta \tag{7.23}$$

The roll response to aileron transfer function is easily derived from equation (7.23). Taking the Laplace transform of that equation, assuming zero initial conditions, and assuming that the rudder is held fixed, $\zeta = 0$, then

$$sp(s) = l_p p(s) + l_\xi \xi(s) \tag{7.24}$$

which, on rearranging, may be written as

$$\frac{p(s)}{\xi(s)} = \frac{l_\xi}{(s - l_p)} \equiv \frac{k_p}{(s + 1/T_r)} \tag{7.25}$$

The transfer function given by equation (7.25) is the approximate reduced order equivalent of the transfer function given by equation (7.3) and is the transfer function of a simple first order lag with time constant T_r. For small perturbation motion, equation (7.25) describes the first one or two seconds of roll response to aileron with a reasonable degree of accuracy; it is especially valuable as a means for identifying the dominant physical properties of the airframe which determine the roll mode time constant. With reference to definitions of the concise aerodynamic stability derivatives in Appendix 2, the roll mode time constant is determined approximately by

$$T_r \cong -\frac{1}{l_p} = -\frac{(I_x I_z - I_{xz}^2)}{\left(I_z \mathring{L}_p + I_{xz} \mathring{N}_p\right)} \tag{7.26}$$

Since $I_x >> I_{xz}$ and $I_z >> I_{xz}$, equation (7.26) may be further simplified to give the classical approximate expression for the roll mode time constant:

$$T_r \cong -\frac{I_x}{\overset{\circ}{L}_p} \tag{7.27}$$

where I_x is the moment of inertia in roll and $\overset{\circ}{L}_p$ is the dimensional derivative describing the aerodynamic damping in roll.

7.3.2 The spiral mode approximation

Since the spiral mode is very slow to develop following a disturbance, it is usual to assume that the motion variables v, p, and r are quasi-steady relative to the time scale of the mode. Whence $\dot{v} = \dot{p} = \dot{r} = 0$, and the lateral-directional state equation (7.1) may be written as

$$\begin{bmatrix} 0 \\ 0 \\ 0 \\ \dot{\phi} \end{bmatrix} = \begin{bmatrix} y_v & y_p & y_r & y_\phi \\ l_v & l_p & l_r & l_\phi \\ n_v & n_p & n_r & n_\phi \\ 0 & 1 & 0 & 0 \end{bmatrix} \begin{bmatrix} v \\ p \\ r \\ \phi \end{bmatrix} + \begin{bmatrix} y_\xi & y_\zeta \\ l_\xi & l_\zeta \\ n_\xi & n_\zeta \\ 0 & 0 \end{bmatrix} \begin{bmatrix} \xi \\ \zeta \end{bmatrix} \tag{7.28}$$

Further, if aircraft wind axes are assumed $l_\phi = n_\phi = 0$, and if the controls are assumed fixed such that unforced motion only is considered, $\xi = \zeta = 0$, equation (7.28) simplifies to

$$\begin{bmatrix} 0 \\ 0 \\ 0 \\ \dot{\phi} \end{bmatrix} = \begin{bmatrix} y_v & y_p & y_r & y_\phi \\ l_v & l_p & l_r & 0 \\ n_v & n_p & n_r & 0 \\ 0 & 1 & 0 & 0 \end{bmatrix} \begin{bmatrix} v \\ p \\ r \\ \phi \end{bmatrix} \tag{7.29}$$

The first three rows in this equation may be rearranged to eliminate the variables v and r to give a reduced-order equation in which the variables are roll rate p and roll angle ϕ only:

$$\begin{bmatrix} 0 \\ \dot{\phi} \end{bmatrix} = \begin{bmatrix} y_v \dfrac{(l_p n_r - l_r n_p)}{(l_r n_v - l_v n_r)} + y_p + y_r \dfrac{(l_v n_p - l_p n_v)}{(l_r n_v - l_v n_r)} & y_\phi \\ 1 & 0 \end{bmatrix} \begin{bmatrix} p \\ \phi \end{bmatrix} \tag{7.30}$$

The first element of the first row of this reduced-order state matrix may be simplified since the terms involving y_v and y_p are assumed to be insignificantly small compared with the term involving y_r. Thus the equation may be rewritten as

$$\begin{bmatrix} 0 \\ \dot{\phi} \end{bmatrix} = \begin{bmatrix} y_r \dfrac{(l_v n_p - l_p n_v)}{(l_r n_v - l_v n_r)} & y_\phi \\ 1 & 0 \end{bmatrix} \begin{bmatrix} p \\ \phi \end{bmatrix} \tag{7.31}$$

Since $\dot{\phi} = p$, equation (7.31) may be reduced to the single degree of freedom equation describing, approximately, the unforced rolling motion involved in the spiral mode:

$$\dot{\phi} + \left(\frac{y_\phi (l_r n_v - l_v n_r)}{y_r (l_v n_p - l_p n_v)} \right) \phi = 0 \tag{7.32}$$

The Laplace transform of equation (7.32), assuming zero initial conditions, is

$$\phi(s)\left(s+\left(\frac{y_\phi(l_r n_v - l_v n_r)}{y_r(l_v n_p - l_p n_v)}\right)\right) \equiv \phi(s)\left(s + 1/T_s\right) = 0 \tag{7.33}$$

It should be noted that equation (7.33) is the reduced order lateral-directional characteristic equation retaining a very approximate description of the spiral mode characteristics only. Whence an approximate expression for the time constant of the spiral mode is defined:

$$T_s \cong \frac{y_r(l_v n_p - l_p n_v)}{y_\phi(l_r n_v - l_v n_r)} \tag{7.34}$$

The spiral mode time constant (7.34) may be expressed conveniently in terms of the dimensional or dimensionless aerodynamic stability derivatives to provide a more direct link with the aerodynamic mode drivers. With reference to Appendix 2 and noting that $Y_{\dot{r}} << mU_e$ and so $y_r \cong -U_e \equiv -V_0$, and that $y_\phi = g$ since aircraft wind axes are assumed, equation (7.34) may be restated as

$$T_s \cong -\frac{U_e\left(\mathring{L}_v \mathring{N}_p - \mathring{L}_p \mathring{N}_v\right)}{g\left(\mathring{L}_r \mathring{N}_v - \mathring{L}_v \mathring{N}_r\right)} \equiv -\frac{V_0(L_v N_p - L_p N_v)}{g(L_r N_v - L_v N_r)} \tag{7.35}$$

A stable spiral mode requires that the time constant T_s is positive. Typically for most aeroplanes, especially in subsonic flight,

$$(L_v N_p - L_p N_v) > 0$$

and the condition for the mode to be stable simplifies to the approximate classical requirement that

$$L_v N_r > L_r N_v \tag{7.36}$$

Further analysis of this requirement is only possible if the derivatives in equation (7.36) are expressed in terms of the aerodynamic properties of the airframe. This means that L_v, dihedral effect, and N_r, damping in yaw, should be large whilst N_v, yaw stiffness, should be small. Rolling moment due to yaw rate, L_r, is usually significant in magnitude and positive. In very simple terms, aeroplanes with small fins and reasonable dihedral are more likely to have a stable spiral mode.

7.3.3 The dutch roll mode approximation

For the purpose of creating a reduced-order model to describe the dutch roll mode, it is usual to make the rather gross assumption that dutch rolling motion involves no rolling motion at all. This is clearly contradictory, but is based on the fact that the mode is first a yawing oscillation and aerodynamic coupling causes rolling motion as a secondary effect. It is probably true that for most aeroplanes the roll to yaw ratio in dutch rolling motion is less than 1 and in some cases may be much less than 1, which gives the assumption some small credibility. Thus the lateral-directional state equation (7.1) may be simplified by writing

$$\dot{p} = p = \dot{\phi} = \phi = 0$$

As before, if aircraft wind axes are assumed, $l_\phi = n_\phi = 0$, and if the controls are assumed fixed such that unforced motion only is considered, $\xi = \zeta = 0$, then equation (7.1) simplifies to

$$\begin{bmatrix} \dot{v} \\ \dot{r} \end{bmatrix} = \begin{bmatrix} y_v & y_r \\ n_v & n_r \end{bmatrix} \begin{bmatrix} v \\ r \end{bmatrix} \tag{7.37}$$

If equation (7.37) is written as

$$\dot{\mathbf{x}}_d = \mathbf{A}_d \mathbf{x}_d$$

then the reduced-order characteristic equation describing the approximate dynamic characteristics of the dutch roll mode is given by

$$\Delta_d(s) = \det[s\mathbf{I} - \mathbf{A}_d] = \begin{vmatrix} s - y_v & -y_r \\ -n_v & s - n_r \end{vmatrix} = 0$$

or

$$\Delta_d(s) = s^2 - (n_r + y_v)s + (n_r y_v - n_v y_r) = 0 \tag{7.38}$$

Therefore, the damping and frequency properties of the mode are given approximately by

$$\begin{aligned} 2\zeta_d \omega_d &\cong -(n_r + y_v) \\ \omega_d^2 &\cong (n_r y_v - n_v y_r) \end{aligned} \tag{7.39}$$

With reference to Appendix 2, the expressions given by equations (7.39) can be restated in terms of dimensional aerodynamic stability derivatives. Further approximating simplifications are made by assuming that $Y_r << mU_e$, so that $y_r \cong -U_e \equiv -V_0$, and by assuming, quite correctly, that both I_x and I_z are usually much greater than I_{xz}. It then follows that

$$\begin{aligned} 2\zeta_d \omega_d &\cong -\left(\frac{\mathring{N}_r}{I_z} + \frac{\mathring{Y}_v}{m} \right) \\ \omega_d^2 &\cong \left(\frac{\mathring{N}_r}{I_z}\frac{\mathring{Y}_v}{m} + V_0 \frac{\mathring{N}_v}{I_z} \right) \cong V_0 \frac{\mathring{N}_v}{I_z} \end{aligned} \tag{7.40}$$

Comparing the damping and frequency terms in the expressions in equations (7.40) with those of the mass-spring-damper in Appendix 6, it is easy to identify the roles of those aerodynamic stability derivatives which are dominant in determining the characteristics of the dutch roll mode. For example, $\mathring{N}_r$ is referred to as the yaw damping derivative and $\mathring{N}_v$ is referred to as the yaw stiffness derivative; both are very dependent on the aerodynamic design of the fin and the fin volume ratio.

Although the dutch roll mode approximation gives a rather poor impression of the real thing, it is useful as a means for gaining insight into the physical behaviour of the mode and its governing aerodynamics.

EXAMPLE 7.2

It has been stated that the principle use of the lateral-directional reduced-order models is to provide insight into the aerodynamic mode drivers. With the exception of the transfer function describing roll rate response to aileron, transfer functions derived from the reduced-order models are not commonly used in analytical work because their accuracy is generally poor. However, it is instructive to compare the values of the mode characteristics obtained from the reduced-order models with those obtained in the solution of the full order equations of motion.

Consider the Douglas DC-8 aircraft of Example 7.1. The equations of motion referred to wind axes are given by equation (7.10), and the solution gives the characteristic equation (7.14). The unfactorised characteristic equation is

$$\Delta(s) = s^4 + 1.5898s^3 + 1.7820s^2 + 1.9200s + 0.0125 = 0 \tag{7.41}$$

In accordance with the expression given in equations (7.21), approximate values for the roll mode and spiral mode time constants are given by

$$\begin{aligned} T_r &\cong \frac{A}{B} = \frac{1}{1.5898} = 0.629\,\text{s} \\ T_s &\cong \frac{D}{E} = \frac{1.9200}{0.0125} = 153.6\,\text{s} \end{aligned} \tag{7.42}$$

The approximate roll mode time constant does not compare particularly well with the exact value of 0.75 seconds, whereas the spiral mode time constant compares extremely well with the exact value of 154 s.

The approximate roll rate response to aileron transfer function, given by equation (7.25), may be evaluated by obtaining the values for the concise derivatives l_p and l_ξ from equation (7.10). Whence

$$\frac{p(s)}{\xi(s)} = \frac{-1.62}{(s + 1.232)}\,\text{deg/s/deg} \tag{7.43}$$

With reference to equation (7.25), an approximate value for the roll mode time constant is given by

$$T_r \cong \frac{1}{1.232} = 0.812\,\text{s} \tag{7.44}$$

which compares rather more favourably with the exact value. The short term roll rate response of the DC-8 to a 1 deg aileron step input, as given by equation (7.43), is shown in Fig. 7.6, where it is compared with the exact response of the full order model, as given by equations (7.12).

Clearly, for the first two seconds, or so, the match is extremely good, which confirms the assumptions made about the mode to be valid provided the period of observation of roll behaviour is limited to the time scale of the roll mode. The approximate roll mode time constant calculated by substituting into the expression given by equation (7.27) the appropriate derivative

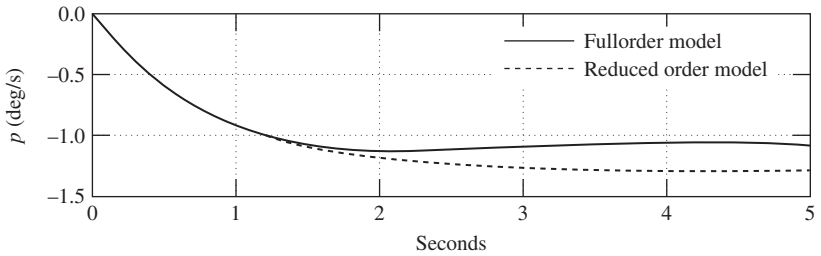

FIGURE 7.6 Roll rate response to a 1 deg aileron step input.

and roll inertia values, given in the aircraft data, results in a value almost the same as that given by equation (7.44). This simply serves to confirm the validity of the assumptions made about the roll mode.

With reference to equations (7.34) and (7.35), the approximate spiral mode time constant may be written in terms of concise derivatives as

$$T_s \cong -\frac{U_e(l_v n_p - l_p n_v)}{g(l_r n_v - l_v n_r)} \tag{7.45}$$

Substituting values for the concise derivatives obtained from equation (7.10), the velocity U_e and g, then

$$T_s \cong -\frac{468.2(0.0002 + 0.00343)}{32.2(0.0011 - 0.00149)} = 135.34\,\text{s} \tag{7.46}$$

Clearly, this approximate value of the spiral mode time constant does not compare so well with the exact value of 154 s. However, this is not so important since the mode is very *slow* in the context of normal piloted manoeuvring activity. The classical requirement for spiral mode stability given by the inequality condition of equation (7.36) is satisfied since $0.00149 > 0.0011$.

Notice how close the values of the two numbers are, suggesting that the mode is close to neutrally stable in the time scale of normal transient response. This observation is quite typical of a conventional aeroplane like the DC-8.

Approximate values for the dutch roll mode damping ratio and undamped natural frequency are obtained by substituting the relevant values for the concise derivatives, obtained from equation (7.10), into the expressions given by equations (7.39). Thus, approximately,

$$\omega_d \cong 1.152\ \text{rad/s}$$
$$\zeta_d \cong 0.135$$

These approximate values compare reasonably well with the exact values, which are a natural frequency of 1.2 rad/s and a damping ratio of 0.11. Such a good comparison is not always

achieved and merely emphasises once more the validity of the assumptions about the dutch roll mode in this particular application. The implication is that at the flight condition of interest the roll-to-yaw ratio of the dutch roll mode in the DC-8 is significantly less than 1 and, indeed, this may be inferred from either Fig. 7.1 or Fig. 7.2.

7.4 Frequency response

It is useful, and sometimes necessary, to investigate the lateral-directional response properties of an aeroplane in the frequency domain. The reasons that such an investigation might be made are much the same as those given for the longitudinal case in Section 6.4. Again, the Bode diagram is the most commonly used graphical tool for lateral-directional frequency response analysis. The method of constructing the diagram and its interpretation follow the general principles described in Section 6.4 and are not repeated here. Since it is difficult to generalise, a typical illustration of lateral-directional frequency response analysis is given in the following example.

EXAMPLE 7.3

The lateral-directional frequency response of the Douglas DC-8 aircraft is evaluated for the same flight condition as in Examples 7.1 and 7.2. The total number of transfer functions which could be evaluated in a Bode diagram is 10, given by equations (7.12) and (7.13), but to create 1 Bode diagrams would be prohibitively lengthy in the present context. Since the essential frequency response information can be obtained from a much smaller number of transfer functions, the present example is limited to 4. The chosen transfer functions were selected from equations (7.12) and (7.13); all are referred to aircraft wind axes and are repeated here for convenience.

$$\begin{aligned}
\frac{\phi(s)}{\xi(s)} &= \frac{-1.62(s^2+0.362s+1.359)}{(s+0.0065)(s+1.329)(s^2+0.254s+1.433)} \text{ rad/rad (deg/deg)} \\
\frac{\beta(s)}{\xi(s)} &= \frac{0.0188(s+0.197)(s-7.896)}{(s+0.0065)(s+1.329)(s^2+0.254s+1.433)} \text{ rad/rad (deg/deg)} \\
\frac{r(s)}{\zeta(s)} &= \frac{-0.864(s+1.335)(s^2-0.03s+0.109)}{(s+0.0065)(s+1.329)(s^2+0.254s+1.433)} \text{ rad/s/rad (deg/s/deg)} \\
\frac{p(s)}{\zeta(s)} &= \frac{0.392s(s+1.85)(s-2.566)}{(s+0.0065)(s+1.329)(s^2+0.254s+1.433)} \text{ rad/s/rad (deg/s/deg)}
\end{aligned} \tag{7.47}$$

The first two transfer functions in equations (7.47) describe lateral response to the lateral command (aileron) variable; the third describes directional response to the directional command (rudder) variable; the fourth was chosen to illustrate cross-coupling and describes lateral response to the directional command variable. Now consider the frequency response of each transfer function in turn.

The frequency response of roll attitude ϕ to aileron input ξ is shown in Fig. 7.7. The most obvious features of the Bode diagram are the very high steady-state gain, 45 dB, and the very

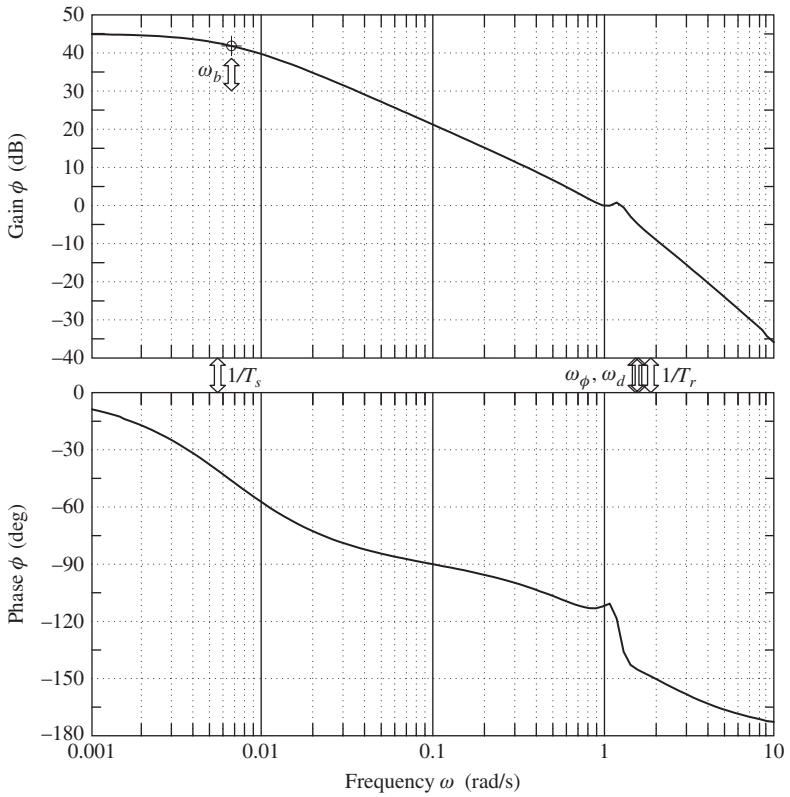

FIGURE 7.7 DC-8 roll attitude frequency response to aileron.

small peak at the dutch roll frequency. The *roll-off* in phase behaves quite conventionally in accordance with the transfer function properties. The high zero frequency gain corresponds with a gain ratio of approximately 180. This means that following a 1 deg aileron step input the aeroplane settles at a roll attitude of −180 degrees—in other words, inverted! Clearly, this is most inappropriate for a large civil transport aeroplane and serves as yet another illustration of the limitations of linear system modelling. Such a large amplitude excursion is definitely not a small perturbation and should not be regarded as such.

Nevertheless, the high zero frequency, or steady-state, gain provides a good indication of roll control sensitivity. As the control input frequency is increased, the attitude response attenuates steadily with increasing phase lag, the useful bandwidth being a little above the spiral mode break frequency $1/T_s$. However, at all frequencies up to that corresponding with the roll subsidence mode break frequency, $1/T_r$, the aeroplane responds to aileron because the gain is always

greater than 0 dB; it is the steady reduction in control sensitivity that will be noticed by the pilot.

Since the dutch roll damping ratio is relatively low at 0.11, an obvious peak might be expected in the gain plot at the dutch roll frequency, but clearly this is not the case. Inspection of the relevant transfer function in equations (7.47) shows that the second order numerator factor very nearly cancels the dutch roll roots in the denominator. This means that the dutch roll dynamics are not very obvious in the roll attitude response to aileron in accordance with the observation. This conclusion is also confirmed by the time history response shown in Fig. 7.1. In fact, the dutch roll cancellation is sufficiently close that it is permissible to write the transfer function in approximate form with little loss of meaning:

$$\frac{\phi(s)}{\xi(s)} = \frac{-1.62}{(s+0.0065)(s+1.329)} \text{ rad/rad (deg/deg)} \tag{7.48}$$

The time response plot and the Bode diagram derived from this approximate transfer function correspond closely with those derived from the full transfer function and may be interpreted to achieve the same conclusions for all practical purposes.

The frequency response of sideslip angle β to aileron input ξ is shown in Fig. 7.8 and corresponds with the second transfer function given in equations (7.47). Again, there are no real surprises here. The transfer function is non-minimum phase since the numerator term $1/T_{\beta_2}$ is negative, which introduces 90 deg of phase lag at the corresponding break frequency. In this response variable the dutch roll gain peak is clearly visible. However, at the dutch roll frequency the gain is attenuated by about -20 dB, which means that the pilot sees no significant oscillatory sideslip behaviour. Again, it is established that the usable bandwidth is a little higher than the spiral mode break frequency $1/T_s$.

The frequency response of yaw rate r to rudder input ζ is shown in Fig. 7.9. This transfer function describes the typical classical directional response to control, and the frequency response, shown in the figure, has some interesting features. The gain plot indicates a steady but significant attenuation with increasing frequency to reach a minimum of about -30 dB at ω_ψ, the resonant frequency of the second-order numerator factor. The gain rises rapidly with a further increase in frequency to reach a maximum of 10 dB at the dutch roll frequency, only to decrease rapidly thereafter.

At very low input frequencies the phase lag increases gently in accordance with the spiral mode dynamics until the effect of the second-order numerator term becomes apparent. The rate of change in phase is then very dramatic since the effective damping ratio of the second-order numerator term is very small and negative. At the dutch roll frequency, approximately, the phase reaches -360 degrees and the response appears to be in phase again, only to roll off smartly at higher frequency. Again, the effective bandwidth is a little higher than the spiral mode break frequency $1/T_s$. These unusual frequency response characteristics are easily appreciated in a flight demonstration.

If the pilot approximates a sinusoidal rudder input by pedalling gently on the rudder pedals, then, at very low frequencies approaching the steady state, the yaw rate response follows the input easily and obviously, since the gain is approximately 20 dB, with very little phase lag. As

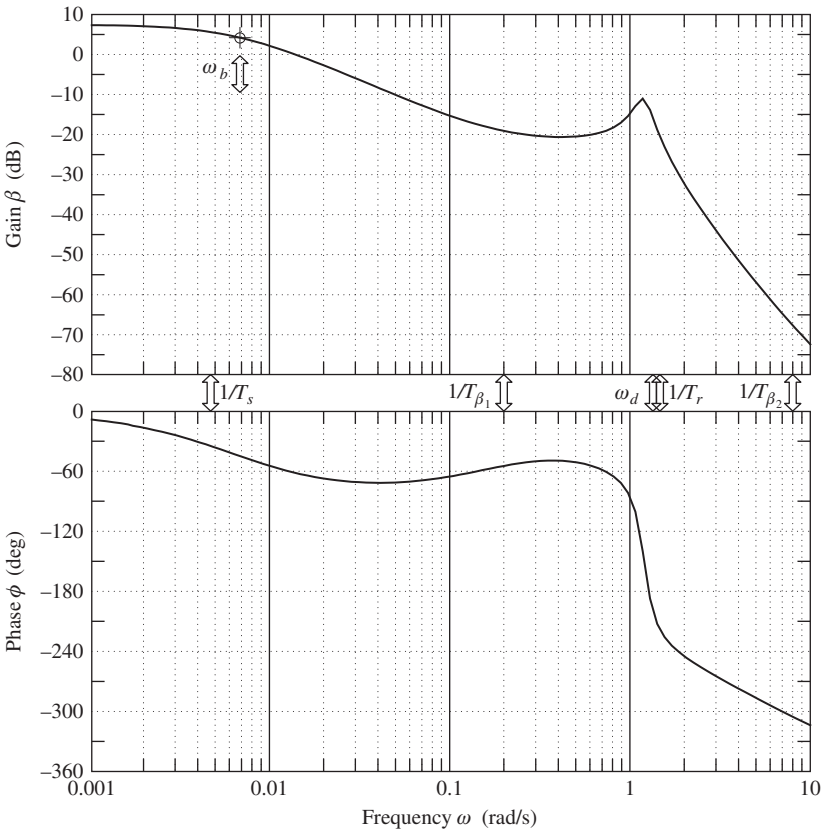

FIGURE 7.8 DC-8 sideslip angle frequency response to aileron.

the pilot increases the frequency of pedalling, the response lags the input and the magnitude of the response reduces very quickly until there is no significant observable response. If the pilot increases the frequency of his forcing yet further, the aircraft springs to life again as the dutch roll frequency (resonance) is reached, at which point the yaw rate response is approximately in phase with the input. At still higher frequencies the response rapidly attenuates for good. The substantial dip in both gain and phase response with frequency, caused by the second-order numerator factor, effectively isolates the dutch roll mode to a small window in the frequency band. This makes it very easy for the pilot to identify and excite the dutch roll mode by rudder pedaling—which is very good for flight demonstration but may not be so good for handling if the dutch roll damping is low and the second-order numerator factor is not too close in frequency to that of the dutch roll mode.

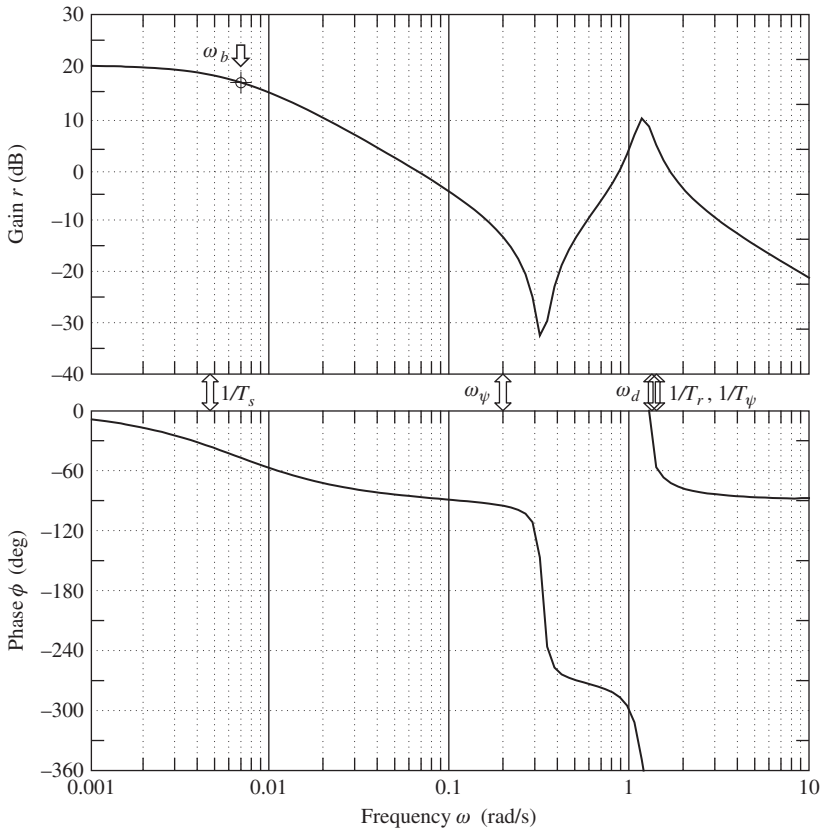

FIGURE 7.9 DC-8 yaw rate frequency response to rudder.

The frequency response of roll rate p to rudder input ζ is shown in Fig. 7.10. This frequency response example is interesting since it represents a cross-coupling case. In the steady state or, equivalently, at zero frequency, roll rate in response to rudder input would not be expected. This is clearly evident in the gain plot, where the gain is $-\infty$ dB at zero frequency. This observation is driven by the zero in the numerator, which also introduces 90 degrees of phase lead at the very lowest frequencies. This zero also very nearly cancels with the spiral mode denominator root such that, at input frequencies above the spiral mode break frequency $1/T_s$, the response in both gain and phase is essentially *flat* until the effects of the remaining numerator and denominator roots come into play, all at frequencies around the dutch roll frequency. The dutch roll resonant peak in gain and the subsequent roll-off in both gain and phase are absolutely classical and easily interpreted. These frequency response observations correspond well with the response time history shown in Fig. 7.2, where the effects of the roll subsidence mode and the dutch roll

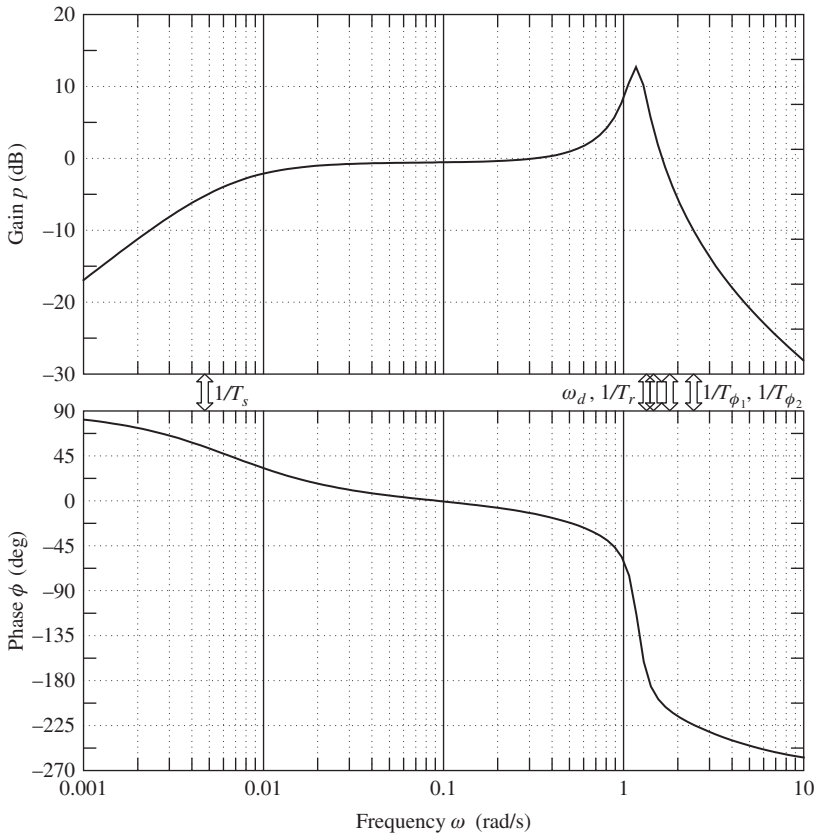

FIGURE 7.10 DC-8 roll rate frequency response to rudder.

mode are clearly visible whilst the longer term convergence associated with the spiral mode is not visible at all. In this example, bandwidth tends to lose its meaning. However, it is not unrealistic to suggest that the usable bandwidth is a little higher than the dutch roll mode frequency, provided the effects at very low frequency are ignored. This then assumes that the zero numerator factor cancels with the spiral mode denominator factor to give the approximate transfer function:

$$\frac{p(s)}{\zeta(s)} = \frac{0.392(s + 1.85)(s - 2.566)}{(s + 1.329)(s^2 + 0.254\,s + 1.433)} \text{ rad/s/rad (deg/s/deg)} \tag{7.49}$$

As before, this may be interpreted in both the time domain and the frequency domain with little loss of meaning over the usable frequency band.

7.5 Flying and handling qualities

As with longitudinal stability, the lateral-directional stability characteristics of the aeroplane are critically important in the determination of flying and handling qualities, and there is no doubt that they must be correct. Traditionally, the emphasis on lateral-directional flying and handling qualities has been much less than the emphasis on longitudinal flying and handling qualities. Unlike longitudinal flying and handling qualities, lateral-directional flying and handling qualities do not usually change significantly with flight condition, especially in the context of small-perturbation modelling. Thus, once they have been fixed by the aerodynamic design of the airframe, they tend to remain more or less constant irrespective of flight condition. Any major lateral-directional departures from nominally small perturbations about trim are likely to be transient, under full pilot control, and consequently are unlikely to give rise to serious handling problems. However, this is not necessarily a safe assumption when considering highly augmented aircraft, a topic which is beyond the scope of the present discussion.

It is a recurrent theme in handling qualities work that short-term dynamics are properly controlled by design. The typical frequencies involved in short-term dynamics are similar to human pilot frequencies, and their inadvertent mismatch is a sure recipe for potential handling problems. So, for reasons similar to those discussed in greater detail in Section 6.5 referring to longitudinal dynamics, it is therefore equally important that the lateral-directional short-period stability modes be properly controlled. This may be interpreted to mean that the damping of both the roll subsidence mode and the dutch roll mode should be adequate.

The roll subsidence mode appears to the pilot as a lag in the response to control and, clearly, if the time constant becomes too large, roll response to control becomes too sluggish. A large roll mode time constant is the direct result of low roll stability, although the mode is usually stable as discussed in Section 7.2.1. Generally, acceptable levels of roll mode stability result in a time constant or roll response lag which is almost imperceptible to the pilot. However, it is quite common to find aircraft in which roll mode damping is inadequate, but it is unusual to find overdamped aircraft.

The spiral mode, being a long-period mode, does not usually significantly influence short-term handling. When it is stable and its time constant is sufficiently long, it has little or no impact on flying and handling qualities, but when it is unstable it manifests itself as a trimming problem because the aeroplane continually attempts to diverge laterally. When its time constant is short, the mode is more unstable and the rate of divergence becomes faster with a corresponding increase in pilot workload. Since the mode is generally so slow to develop, the motion cues associated with it may well be imperceptible to the pilot. Thus a hazardous situation may easily arise if the external visual cues available to the pilot are poor or absent altogether, such as in Instrument Meteorological Conditions (IMC) flight conditions. It is not unknown for inexperienced pilots to become disorientated in such circumstances, with the inevitable outcome! Therefore, the general requirement is that the spiral mode should be stable; however, since this is difficult to achieve in many aeroplanes, when unstable the time constant should be greater than a defined minimum.

Since the dutch roll mode is a short-period mode and is the directional equivalent of the longitudinal short-period mode, its importance to handling is similarly critical. Generally, it is essential that the dutch roll mode is stable and that its damping is greater than a defined minimum. Similarly

tight constraints are placed on the permitted range of combinations of frequency and damping. However, a level of damping lower than that of the longitudinal short-period mode is permitted. This is perhaps convenient but is more likely to result from the design conflict with the spiral mode, which must not have more than a limited degree of instability.

7.6 Mode excitation

Unlike the longitudinal stability modes, the lateral-directional stability modes usually exhibit significant dynamic coupling; as a result, it is more difficult to excite the modes independently for the purposes of demonstration or measurement. However, the lateral-directional stability modes may be excited selectively by the careful application of a sympathetic aileron or rudder input to the trimmed aircraft. Again, the methods developed for in-flight mode excitation reflect an intimate understanding of the dynamics involved and are generally easily adapted to the analytical environment. Because the lateral-directional stability modes usually exhibit dynamic coupling, the choice and shape of the disturbing input are critical to the mode under investigation. As always, standard experimental procedures have been developed to achieve consistency in the flight test or analytical process so that meaningful comparative studies may be carried out.

The roll subsidence mode may be excited by applying a short duration square pulse to the aileron with the other controls remaining fixed at their trim settings. The magnitude and duration of the pulse must be carefully chosen if the aeroplane is not to roll too rapidly through a large attitude change and thereby exceed the limit of small-perturbation motion. Since the mode involves almost pure rolling motion only, no significant motion coupling is seen in its relatively short time scale. Therefore, to see the classical characteristics of the roll subsidence mode it is only necessary to observe roll response for a few seconds.

An example of roll response showing the roll subsidence mode recorded during a flight test exercise in a Handley Page Jetstream aircraft is shown in Fig. 7.11. The input aileron pulse is clearly seen and has a magnitude of about 4 deg and duration of about 4 s. The shape of this input will have been established by the pilot by trial and error since the ideal input is very much aircraft dependent. The effect of the roll mode time constant, is clearly visible since it governs the exponential rise in roll rate p as the response attempts to follow the leading edge of the input ξ. The same effect is seen again in reverse when the input is returned to its datum at the end of the pulse. The barely perceptible oscillation in roll rate during the "steady part" of the response is, in fact, due to a small degree of coupling with the dutch roll mode.

To conduct the flight experiment without large excursions in roll attitude ϕ, it is usual to first establish the aircraft in a steady turn with, in this illustration, -30 degrees of roll attitude. On application of the input pulse, the aircraft rolls steadily through to $+30$ degrees of roll attitude when the motion is terminated by returning the aileron to datum. This can be seen in Fig. 7.11. The effect of the roll mode time constant on the roll attitude response is to smooth the entry to, and exit from, the steady part of the response. Since the roll mode time constant is small, around 0.4 s for the Jetstream, its effect is only just visible in the roll attitude response. It is interesting to observe that the steady part of the roll response is achieved when the moment due to damping in roll becomes established at a value equal and opposite to the disturbing moment in roll caused by

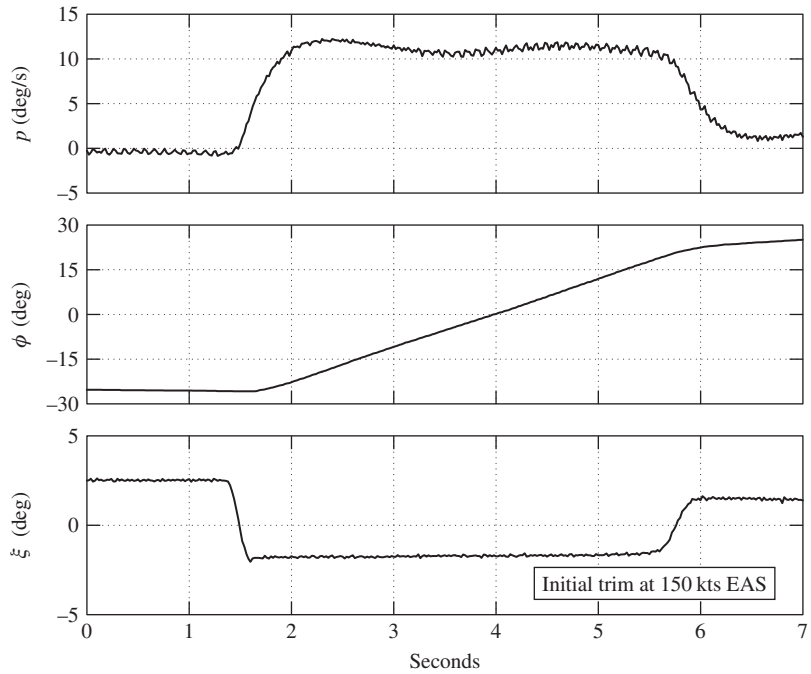

FIGURE 7.11 Flight recording of the roll subsidence mode.

aileron deflection. Clearly, therefore, the roll subsidence mode governs the transient entry to, and exit from, all rolling motion.

The spiral mode may be excited by applying a small step input to rudder ζ, with the remaining controls being held at their trim settings. The aeroplane responds by starting to turn, the wing on the inside of the turn starts to drop, and sideslip develops in the direction of the turn. When the roll attitude reaches about 20 degrees the rudder is gently returned to datum and the aeroplane is left to its own devices. When the spiral mode is stable the aeroplane slowly recovers wings level flight, the recovery being exponential with spiral mode time constant. When the mode is unstable the coupled roll-yaw-sideslip departure continues to develop exponentially with spiral mode time constant.

An example of an unstable spiral mode, captured from the time the disturbing rudder input is returned gently to datum and recorded during a flight test exercise in a Handley Page Jetstream, is shown in Fig. 7.12. The slow exponential divergence is clearly visible in all recorded variables, with the possible exception of sideslip angle β, which is rather noisy. In any event, the magnitude of sideslip is normally limited to a small value by the weathercock effect of the fin. Although speed and altitude play no part in determining the characteristic of the mode, the exponential departure in these variables is a classical, and very visible, consequence of an unstable spiral mode. Once excited, since the aircraft is no longer in wings-level flight, lift is insufficient to maintain altitude and so an accelerating descent follows and the spiral flight path is determined by the mode's

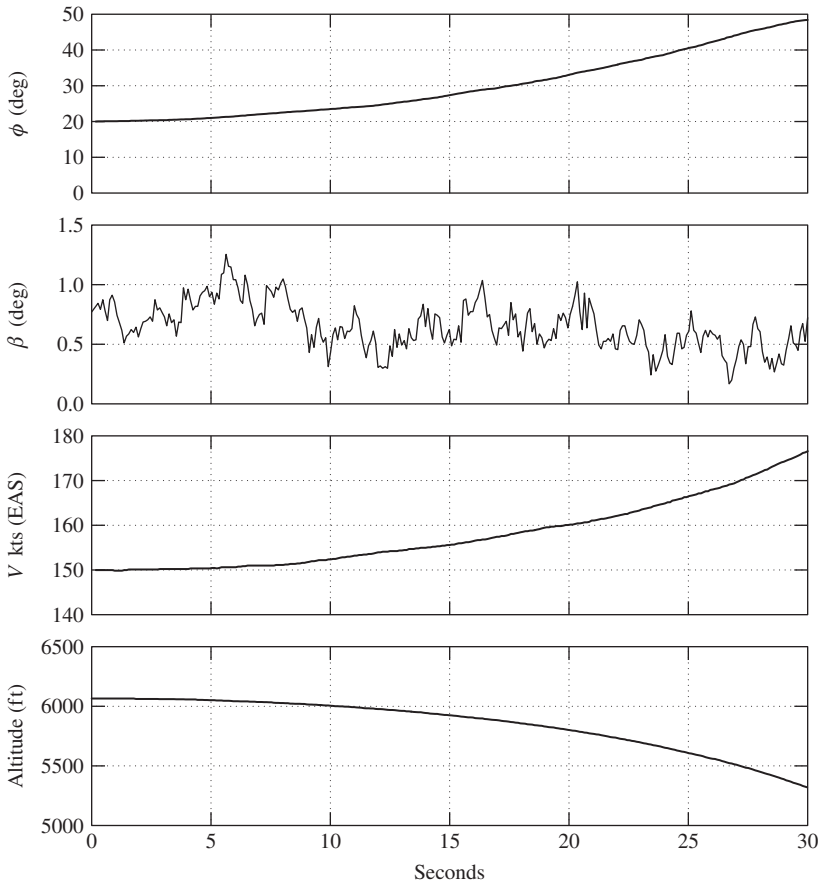

FIGURE 7.12 Flight recording of the spiral mode departure.

aeromechanics of the mode. The first 30 s of the descent is shown in Fig. 7.12. Obviously, the departure must be terminated after a short time if the safety of the aeroplane and its occupants are not to be jeopardised.

Ideally, the dutch roll mode may be excited by applying a doublet to the rudder pedals with a period matched to that of the mode, with all other controls remaining at their trim settings. In practice the pilot pedals continuously and cyclically on the rudder pedal, and by adjusting the frequency it is easy to find the resonant condition. (See the related comments in Example 7.3 and note that the dutch roll frequency is comfortably within the human bandwidth.) In this manner a forced oscillation may easily be sustained. On ceasing the forcing input, the free transient characteristics of the dutch roll mode may be seen. This free response is shown in the flight recording in Fig. 7.13, which was made in a Handley Page Jetstream. The rudder input ζ shows the final doublet before ceasing the forcing at about 5 s; the obvious oscillatory rudder motion after 5 s is due to the cyclic

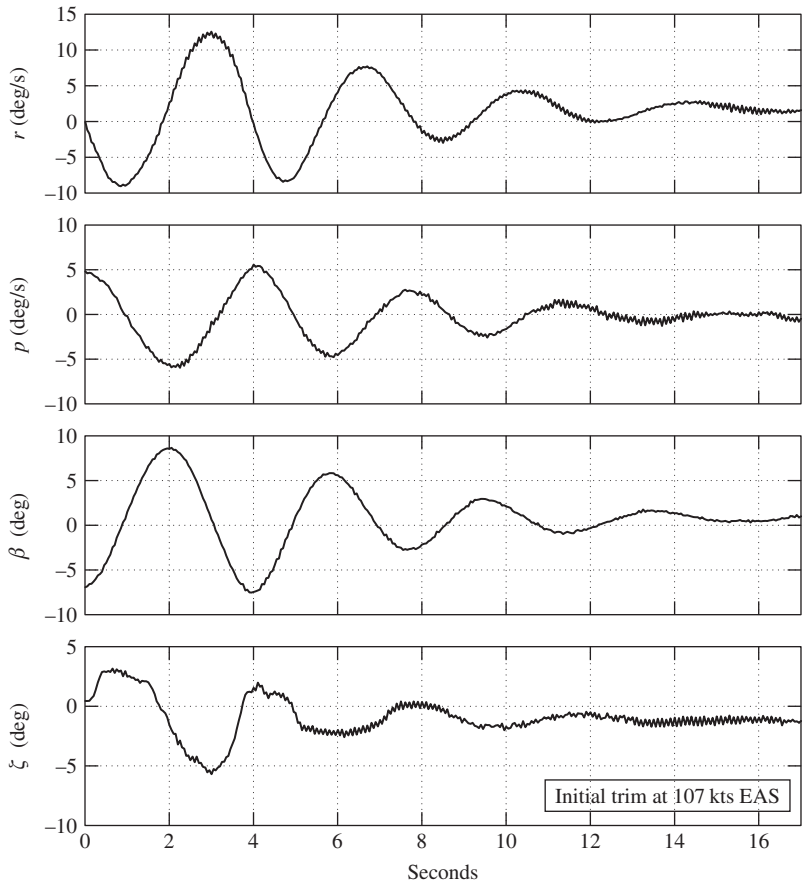

FIGURE 7.13 Flight recording of the dutch roll mode.

aerodynamic load on the free rudder. The classical damped oscillatory motion is clearly visible in the variables shown: yaw rate r, roll rate p, and sideslip angle β. The motion would also be clearly evident in both roll and yaw attitude variables, which are not shown. Note the relative magnitudes of, and the phase shift between, yaw rate r and roll *r*ate p, observations which are consistent with the classical physical explanation of the mode dynamics.

As for the longitudinal modes discussed in Section 6.6, the above flight recordings of the lateral-directional stability modes illustrate the *controls-free* dynamic stability characteristics. The same exercise could be repeated with the controls held fixed following the disturbing input. Obviously, in this event the *controls-fixed* dynamic stability characteristics would be observed and, in general, the differences between the responses would be small. To reiterate the important comments made in Section 6.6, controls-free dynamic response is only possible in aeroplanes with reversible controls, which includes most small classical aeroplanes.

Virtually all larger modern aircraft have powered controls, driven by electronic flight control systems, which are effectively irreversible. This means that they are only capable of exhibiting controls-fixed dynamic response. For this reason, most theoretical modelling and analysis today is concerned only with controls-fixed dynamics, as is the case throughout this book. However, a discussion of the differences between controls-fixed and controls-free aeroplane dynamics may be found in Hancock (1995).

When it is required to investigate analytically the dynamics of a single mode in isolation, the best approach is to emulate flight test practice as much as possible. It is necessary to choose the most appropriate transfer functions to show the dominant response variables in the mode of interest. For example, the roll subsidence mode may only be observed sensibly in the dominant response variable p and, to a lesser extent, in ϕ. Similarly for the spiral and dutch roll modes, it is important to observe the motion in the dominant variables, and hence the most visible in the mode dynamics. It is also essential to apply a control input disturbance sympathetic to the mode dynamics, and it is necessary to observe the response for an appropriate period of time. Otherwise, the dynamics of interest are inevitably obscured by motion coupling effects. For example, Fig. 7.11 shows both the roll subsidence mode and the dutch roll mode, but the excitation, the choice of output variables, and the time scale were chosen to optimise the recording of the roll subsidence mode. The form of control input is not usually difficult to arrange in analytical work since most software packages have built-in impulse, step, and pulse functions, whilst more esoteric functions can usually be programmed by the user. For the analysis of lateral-directional mode dynamics especially, this kind of informed approach is critical if the best possible visualisation of the modes and their associated dynamics are to be obtained.

References

Hancock, G. J. (1995). *An introduction to the flight dynamics of rigid aeroplanes.* Ellis Horwood.

Teper, G. L. (1969). *Aircraft stability and control data.* STI Technical Report 176-1. Hawthorne, CA: Systems Technology, Inc, Nasa Contractor Report, National Aeronautics and Space Administration, Washington D.C. 20546.

PROBLEMS

7.1 Describe the possible modes of lateral-directional motion of an aircraft when disturbed slightly from steady flight.

An aircraft in steady horizontal flight is disturbed slightly in the lateral plane. If the inertia forces associated with the angular accelerations in the resulting motion are neglected, as well as the components of the acceleration and aerodynamic forces along the oy axis, show that the resulting motion is either a divergence or a subsidence depending in general on the sign of $(L_v N_r - L_r N_v)$. Describe how the stability of an aircraft in this mode changes with an increase in fin size.

(CU 1979)

7.2 A transport aircraft whose wing span is 35.8 m is flying at 262 kts at an altitude where the lateral relative density parameter $\mu_2 = 24.4$. The dimensionless controls-fixed lateral-directional characteristic equation is

$$\lambda^4 + 5.8\lambda^3 + 20.3\lambda^2 + 79.0\lambda + 0.37 = 0$$

(a) What can be deduced about the lateral-directional stability of the aircraft from inspection of the characteristic equation?
(b) Solve the characteristic equation approximately; determine estimates for the time constants of the nonoscillatory modes and the frequency and damping ratio of the oscillatory mode.
(c) Comment on the acceptability of this aircraft.

(CU 1980)

7.3 Answer the following questions:
(a) What is the lateral-directional weathercock stability of an aircraft?
(b) State the main aerodynamic contributions to weathercock stability.

(CU 1982)

7.4 The Navion is a small light aeroplane of conventional layout and in a low speed level flight condition, the coefficients of the dimensionless lateral-directional stability quartic are given by

$$\lambda^4 + B_2\lambda^3 + C_2\lambda^2 + D_2\lambda + E_2 = 0$$

where
$B_2 = 20.889$
$C_2 = 46.714\text{-}k_v$
$D_2 = 115.120 - 18.636k_v$
$E_2 = 55.570 + 1.994k_v$

and

$$k_v = -\frac{\mu_2 N_v}{i_z}$$

The lateral relative density parameter $\mu_2 = 11.937$, and the dimensionless moment of inertia in yaw $i_z = 0.037$. The quartic factorises to

$$(\lambda + B_2)\left(\lambda + \frac{E_2}{D_2}\right)(\lambda^2 + k_1\lambda + k_2) = 0$$

Show that if the fin were made too large, the aircraft would become dynamically unstable. What would happen to the aircraft if a critical value were exceeded?

(CU 1983)

7.5 Describe and explain the physical characteristics of the roll subsidence stability mode. Assuming that the motion associated with the mode comprises pure rolling only, write the equation of motion assuming the rudder to be fixed ($\zeta = 0$). By taking the Laplace transform of this equation, show that the roll control transfer function is given by

$$\frac{p(s)}{\xi(s)} = \frac{-k}{(1 + sT_r)}$$

where $k = \overset{\circ}{L}_{\xi} / \overset{\circ}{L}_{p}$ and $T_r = -I_x / \overset{\circ}{L}_{p}$. State any assumptions made in obtaining the transfer function.

(a) Obtain the inverse Laplace transform of the transfer function to show that the roll rate response to a unit step of aileron is given by

$$p(t) = -k\left(1 - \mathrm{e}^{-\frac{t}{T_r}}\right)$$

(b) The Republic F-105 Thunderchief aircraft has a wing span of 10.4 m and a moment of inertia in roll of 13965 kg/m^2. In a cruise flight condition at Mach 0.9 at an altitude of 35,000 ft, the dimensionless derivatives have the following values: $L_p = -0.191$ and $L_{\xi} = -0.029$. Sketch the roll rate response to a 1° step of aileron deflection and comment on the roll handling of the aircraft.

(CU 1986)

7.6 The aircraft described below is flying at a true airspeed of 150 m/s at sea level. At this flight condition it is required to have a steady roll rate of 60 deg/s, when each aileron is deflected through 10 degrees. Assuming that the outboard edges of the ailerons are at the wing tip, calculate the required aileron span. If the ailerons produce 17,500 Nm of adverse yawing moment, calculate the rudder deflection required for trim.

Aircraft data:

Rectangular unswept wing		Fin	
	Span = 15 m		Area = 3 m^2
	Area = 27 m^2		Moment arm from cg = 6 m
	$L_p = -0.2$	Rudder	Area = 1.2 m^2
Aileron	$dC_L/d_{\xi} = 2$ 1/rad		$dC_L/d_{\zeta} = 2.3$ 1/rad

(LU 2001)

7.7 Using a simple model, show that the time to half-amplitude of the roll subsidence mode may be approximated by

$$t_{\frac{1}{2}} = -\frac{I_x}{\overset{\circ}{L}_p}\ln(2)$$

Given that the rolling moment due to roll rate derivative may be written as

$$\overset{\circ}{L}_p = -\rho V_0 \int_0^s \left(C_D + \frac{\mathrm{d}C_L}{\mathrm{d}\alpha} \right)_y c_y y^2 \mathrm{d}y$$

determine the time to half amplitude of the roll subsidence mode for an aircraft with the following characteristics when it is flying at sea level at 100 m/s.

Wing span = 10 m	$\mathrm{d}C_L/\mathrm{d}\alpha$ at root = 5.7 1/rad
Wing root chord = 1.5 m	$\mathrm{d}C_L/\mathrm{d}\alpha$ at tip = 5.7 1/rad
Wing tip chord = 0.75 m	$C_D = 0.005$ (constant)
Inertia in roll = 8000 kg/m^2	

Assume that $\mathrm{d}C_L/\mathrm{d}\alpha$ varies linearly along the span.

(LU 2002)

7.8 For the aircraft described below, determine the value of wing dihedral required to make the spiral mode neutrally stable. The rolling moment due to sideslip derivative is given by

$$L_v = -\frac{1}{Ss} \int_0^s c_y a_y \Gamma y \mathrm{d}y$$

and the time to half (double) amplitude for the spiral mode is given by

$$t_{\frac{1}{2}} = \frac{V_0}{g} \left(\frac{L_v N_p - L_p N_v}{L_v N_r - L_r N_v} \right) \ln(2)$$

Aircraft data:

Wing area	$S = 52$ m^2
Wing span	$B = 14.8$ m
Wing root chord	5.0 m
Wing tip chord	2.0 m
Fin area	$S_F = 8.4$ m^2
Fin roll arm	$h_F = 1.8$ m
Wing lift curve slope	$a_y = 3.84$ 1/rad
Fin lift curve slope	$a_{1F} = 2.2$ 1/rad
L_r	−0.120
N_r	−0.120
N_v	0.158

Discuss how the geometry of the wing and fin influence the stability of the spiral mode.

(LU 2003)